Recent Developments in the Modelling of Neutron-Star Crusts (Personal View)

OUTER LAYER
1 meter thick
solid or liquid

CORE
10-15 kilometer deep
liquid

CRUST
1 kilometer thick
solid

Nicolas Chamel

Institute of Astronomy and Astrophysics
Université Libre de Bruxelles, Belgium

NEUTRON STAR

Catania, 7 November 2017

Prelude

Even though the crust of a neutron star represents about 1% of the
stellar mass and 10% of the radius, it is thought to be related to
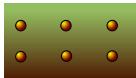various astrophysical phenomena:

- pulsar sudden spin-ups,
- X-ray (super)bursts,
- r-process nucleosynthesis in neutron-star mergers,
- thermal relaxation in transiently accreting stars,
- quasiperiodic oscillations in soft gamma-ray repeaters,
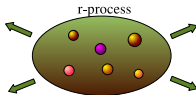- gravitational wave emission (mountains)

Credit: NASA's Goddard Space Flight Center/S. Wiessinger
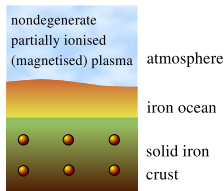
Various neutron star crusts
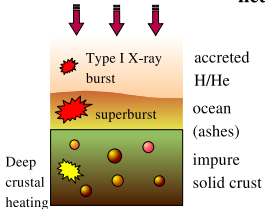

body centered cubic
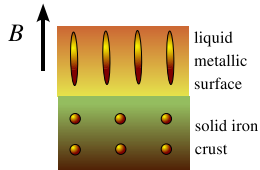crystal of iron

**Low density cold
catalyzed matter**

r-process

**Ejected cold decompressed
neutron star crust matter**

nondegenerate
partially ionised
(magnetised) plasma — atmosphere

iron ocean

solid iron
crust

**Weakly magnetised
neutron star surface**

accreted
H/He

Type I X-ray
burst

ocean
(ashes)

superburst

impure
solid crust

Deep
crustal
heating

**Accreting neutron
star surface**

B

liquid
metallic
surface

solid iron
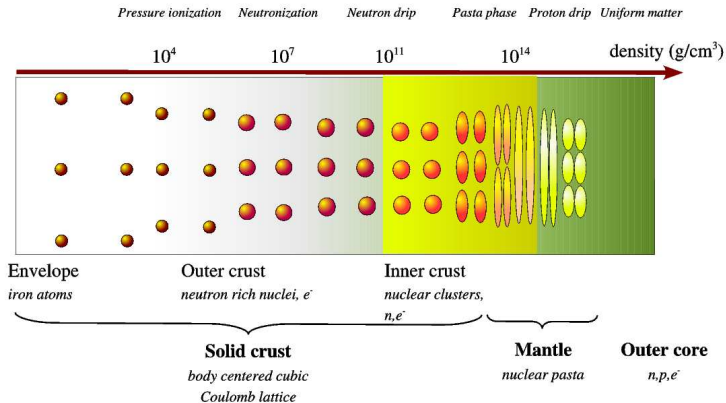crust

**Strongly magnetised
neutron star surface**

# Internal constitution of neutron-star crusts

Chamel&Haensel, Living Reviews in Relativity 11 (2008), 10

The crust exhibits various phases but with *e*, *p*, *n* only: its properties can be fully determined by known atomic and nuclear physics.

Structure of the outermost layers

The surface of a neutron star is made of **iron, the end product of stellar nucleosynthesis** (identification of broad Fe K emission lines from accretion disk around neutron stars in LMXB).

*Stixrude, Phys. Rev. Lett. 108, 055505 (2012)*
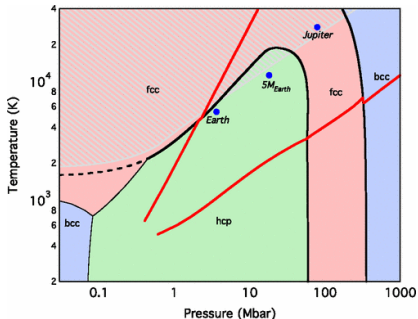
Compressed iron can be studied with **nuclear explosions and laser-driven shock-wave experiments**... but at pressures corresponding to about 0.1 mm below the surface of a neutron star with a mass $\mathcal{M} = 1.4\mathcal{M}_\odot$ and a radius $R = 12$ km !

Ab initio calculations predict various **structural phase transitions**.

Crystal Coulomb plasma

At a density $\rho_{\mathrm{eip}} \approx 2 \times 10^4$ g cm^{-3} (about 22 cm below the surface), the interatomic spacing becomes comparable with the atomic radius.
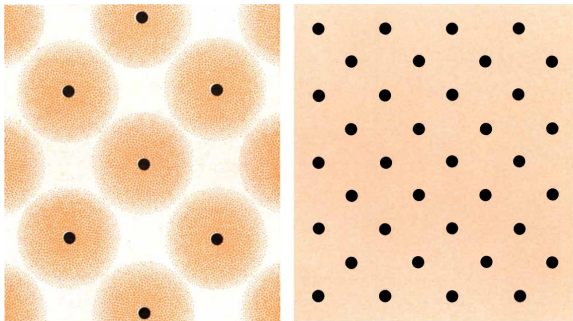
*Ruderman, Scientific American 224, 24 (1971)*

- At densities $\rho \gg \rho_{\mathrm{eip}}$, atoms are crushed into a **dense plasma of nuclei and free electrons**.
- Nuclei form a body-centered cubic (bcc) lattice crystal.

Accreted crust

The composition of the surface layers may be changed by

- the fallback of material from the supernova explosion,
- the accretion of matter from a stellar companion (X-ray bursts).

The equilibrium structure of multicomponent plasmas is uncertain
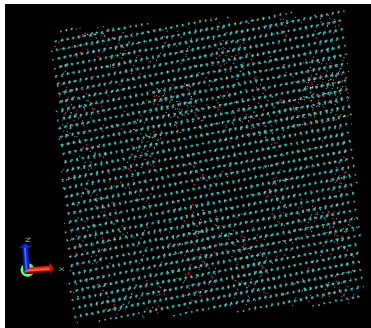
Classical molecular dynamics simulations predict the formation of a **regular crystal or polycrystals**.

However, the system may have not fully relaxed to its true equilibrium.

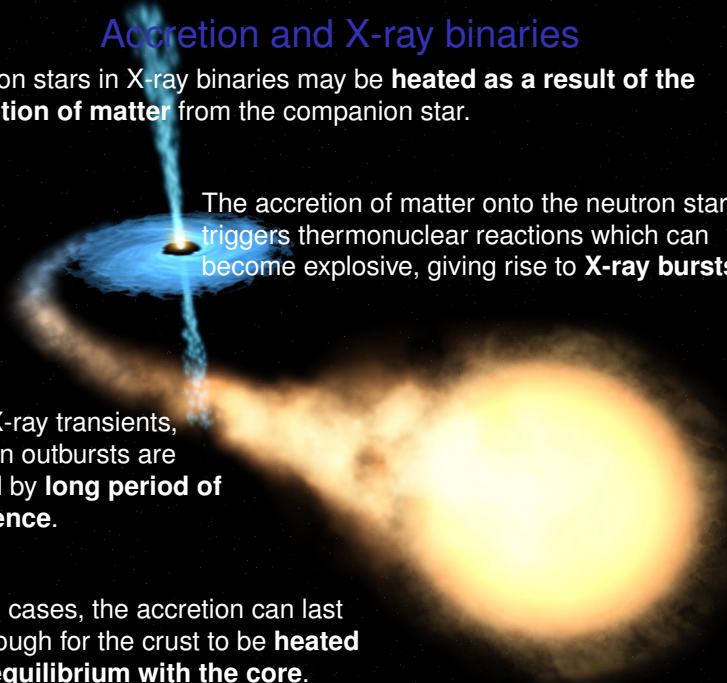Search of the equilibrium structure using genetic algorithms but restricted to O-Fe-S and Fe-As-Se.
Engstrom et al., ApJ.818, 183 (2016)

Horowitz,Berry, Phys.Rev.C79, 065803 (2009)
Horowitz et al., Phys.Rev.E79, 2 (2009)

Accretion and X-ray binaries

Neutron stars in X-ray binaries may be **heated as a result of the accretion of matter** from the companion star.

The accretion of matter onto the neutron star triggers thermonuclear reactions which can become explosive, giving rise to **X-ray bursts**.

In soft X-ray transients, accretion outbursts are followed by **long period of quiescence**.

In some cases, the accretion can last long enough for the crust to be **heated out of equilibrium with the core**.

Thermal relaxation of soft x-ray transients

The thermal relaxation during the quiescent state has been monitored for a few accreting neutron stars.

Waterhouse et al., MNRAS 456, 4001 (2016)
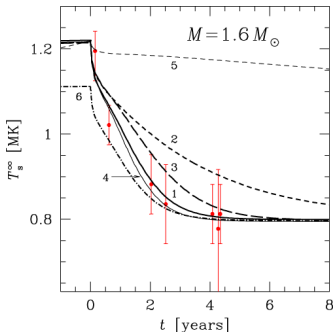
Example: KS 1731−260

Curves 1,3,4 : crystalline crust with neutron superfluidity
Curve 2 : crystalline crust without neutron superfluidity
Curve 4 : perfect crystal with weak neutron superfluidity
Curve 5 : amorphous crust with neutron superfluidity

Shternin et al., MNRAS,L43382(2007)
Brown&Cumming, ApJ698,1020 (2009)

Page&Reddy, Neutron Star Crust, eds Bertulani&Piekarewicz (Nova Science Publishers,New York, 2012) p. 281.

Observations indicate that accreted crusts are not amorphous solids.

Highly-magnetised crust

The electron motion perpendicular to $\boldsymbol{B}$ is quantised into Landau orbitals with a characteristic scale $a_m = a_0\sqrt{B_{\mathrm{at}}/B}$, where a_0 is the Bohr radius

For $B \gg B_{\mathrm{at}} = m_e^2 e^3 c/\hbar^3 \simeq 2.35 \times 10^9$ G, atoms are expected to adopt a very elongated shape along $\boldsymbol{B}$ and to form linear chains
Ruderman, PRL27, 1306 (1971); Medin&Lai, Phys.Rev. A74, 062508 (2006)

The attractive interaction between these chains could lead to a transition into a **condensed phase** with a surface density

$$\rho_s \sim 560 A Z^{-3/5}(B/10^{12}\text{ G})^{6/5}\text{ g cm}^{-3}$$

In deeper regions of the crust,

$$\rho \approx \rho_s \left(1 + \sqrt{\frac{P}{P_0}}\right), \quad P_0 \simeq 1.45 \times 10^{20}(B/10^{12}\text{ G})^{7/5}\left(\frac{Z}{A}\right)^2\text{ dyn cm}^{-2}$$

Lai, Rev.Mod.Phys.73, 629 (2001); Chamel et al., Phys.Rev.C86, 055804 (2012)
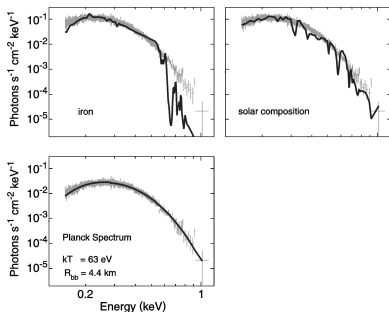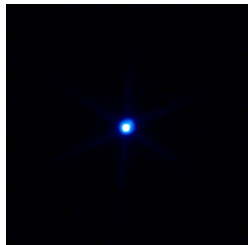
The intriguing case of RX J1856.5-3754

Fig. 3: The Chandra LETG X-ray spectrum of RX J1856 fitted with (non-magnetic) photospheric models assuming pure iron and solar composition. The best fit is obtained with a Planck spectrum (Burwitz et al. 2003).

X-ray observations with Chandra

Turolla et al., ApJ 603, 265 (2004)
van Adelsberg et al., ApJ 628, 902 (2005)
Trümper (2005), astro-ph/0502457

Recent review: *Potekhin et al., Space Sci. Rev. 191, 171 (2015)*

The thermal X-ray emission is best fitted by a black body spectrum: evidence for a condensed surface? The presence of high **B** has found additional support from recent optical polarimetry measurements.
Mignani et al., MNRAS 465, 492 (2017)

Description of the outer crust of a neutron star

Main assumptions:

- cold "catalysed" matter (full thermodynamic equilibrium)
  Harrison, Wakano and Wheeler, Onzième Conseil de Physique Solvay (Stoops, Brussels, Belgium, 1958) pp 124-146

- the crust is stratified into pure layers made of nuclei $^A_Z X$

- electrons are uniformly distributed and are highly degenerate
  $T < T_F \approx 5.93 \times 10^9 (\gamma_r - 1)$ K

  $$\gamma_r \equiv \sqrt{1 + x_r^2}, \qquad x_r \equiv \frac{p_F}{m_e c} \approx 1.00884 \left(\frac{\rho_6 Z}{A} \right)^{1/3}$$

- nuclei are arranged on a perfect body-centered cubic lattice
  $$T < T_m \approx 1.3 \times 10^5 Z^2 \left(\frac{\rho_6}{A} \right)^{1/3} \text{ K} \qquad \rho_6 \equiv \rho / 10^6 \text{ g cm}^{-3}$$

  Tondeur, A&A 14, 451 (1971)
  Baym, Pethick, Sutherland, ApJ 170,299(1971).

Neutron-star crust and nuclear masses

The ground-state composition of the outer crust is completely determined by **nuclear masses** $M'(A, Z)$.

In the limit of ultrarelativistic electron Fermi gas:

$$P_{1\rightarrow 2} \approx \frac{(\mu_e^{1\rightarrow 2})^4}{12\pi^2(\hbar c)^3}, \quad \bar{n}_1^{\max} \approx \frac{A_1}{Z_1}\frac{(\mu_e^{1\rightarrow 2})^3}{3\pi^2(\hbar c)^3}, \quad \bar{n}_2^{\min} \approx \frac{A_2}{Z_2}\frac{Z_1}{A_1}\bar{n}_1^{\max}$$

$$\mu_e^{1\rightarrow 2} \equiv \left[\frac{M'(A_2, Z_2)c^2}{A_2} - \frac{M'(A_1, Z_1)c^2}{A_1}\right]\left(\frac{Z_1}{A_1} - \frac{Z_2}{A_2}\right)^{-1} + m_e c^2$$

Since $\bar{n}_2^{\min} > \bar{n}_1^{\max}$ in hydrostatic equilibrium, matter becomes more **neutron rich** ($Z_2/A_2 < Z_1/A_1$) with increasing depth.

Essentially exact **analytical expressions** valid for any degree of relativity of the electron gas and including electrostatic correction:
Chamel&Fantina,Phys.Rev.C94,065802(2016)

Experimental "determination" of the outer crust

The composition of the crust is completely determined by experimental nuclear masses down to about 200m for a $1.4 M_\odot$ neutron star with a 10 km radius
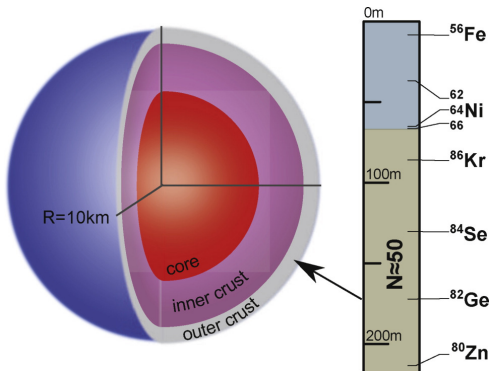
The physics governing the structure of atomic nuclei (magicity) leaves its imprint on the composition.

Due to β equilibrium and electric charge neutrality, Z is more tightly constrained than N: only a few layers with $Z = 28$.

Kreim, Hempel, Lunney, Schaffner-Bielich, Int.J.M.Spec.349-350,63(2013)

Plumbing neutron stars to new depths

Precision measurements of the mass of short-lived zinc nuclides by the ISOLTRAP collaboration at CERN's ISOLDE radioactive-beam facility has recently allowed to "drill" deeper into the crust.
Wolf et al.,PRL110,041101(2013)

The composition is very sensitive to small corrections such as electron screening.
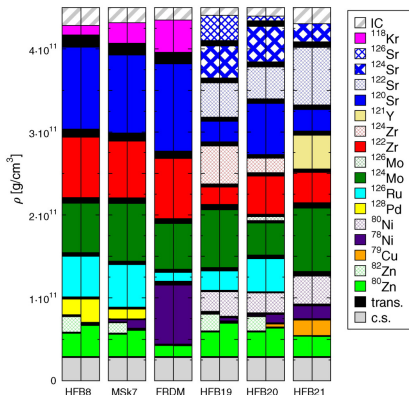*Chamel&Fantina,Phys.Rev.D93,063001(2016)*

Errors on nuclear masses of a few keV can also change the composition!
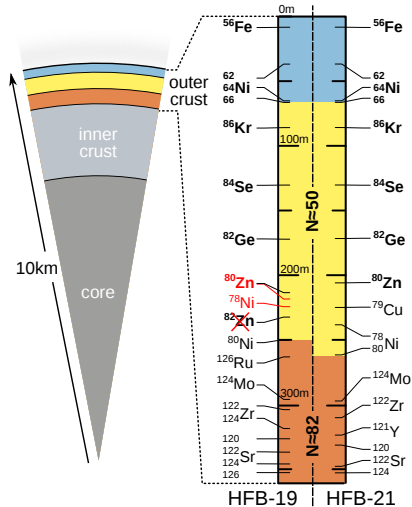
Theoretical predictions of the outer crust

Deeper in the crust, recourse must be made to nuclear mass models:
- semi-empirical formulas (e.g. Bethe & Weizsäcker) – $\sigma \sim 3$ MeV
- mic-mac models (e.g. Duflo & Zucker, FRDM) – $\sigma \sim 0.3$-0.5 MeV
- "microscopic" models (e.g. HFB, RMF) – $\sigma \sim 0.5$-1.5 MeV

Some recent calculations:

Pearson et al.,Phys.Rev.C83,065810(2011)
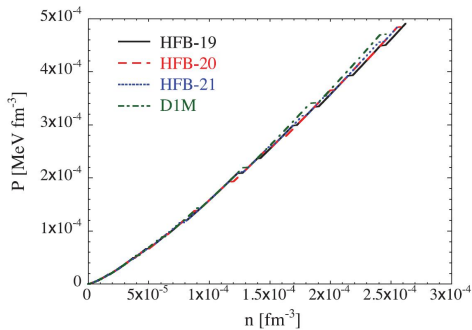*Kreim et al.,Int.J.M.Spec.349-350,63(2013)*
Sharma et al., A&A 584, A103 (2015)
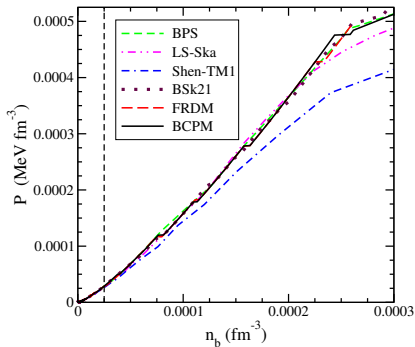*Utama et al., Phys.Rev.C93,014311(2016).*

Although less accurate, microscopic models can also be used to describe the inner crust and the core of a neutron star.

Equation of state of the outer crust

The pressure, dominated by that of the electron Fermi gas, is almost independent of the composition.
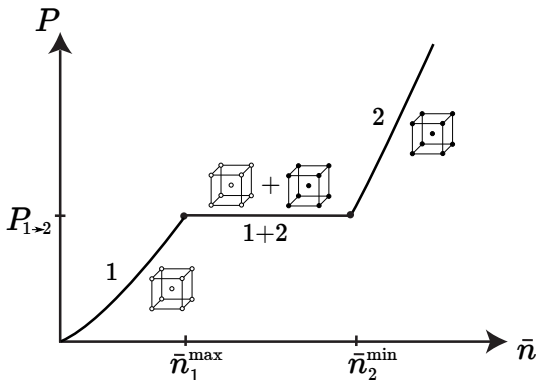

Pearson et al.,Phys.Rev.C83,065810(2011)   *Sharma et al., A&A 584, A103 (2015)*

Stratification and equation of state

Transitions between adjacent crustal layers are accompanied by **density discontinuities.**

Mixed solid phases cannot exist in a neutron star crust because P has to increase strictly monotonically with $\bar{n}$ (hydrostatic equilibrium).

Compounds in neutron-star crusts?

Multinary ionic compounds made of nuclei with charges $\{Z_i\}$ might exist in the crust of a neutron star.
Dyson, Ann. Phys.63, 1 (1971); Witten, ApJ 188, 615 (1974)

Necessary conditions:

- **stability against weak and strong nuclear processes**.
  Jog&Smith, ApJ 253, 839(1982)
- **stability against the separation into pure (bcc) phases**:

$$\mathcal{R}(\{Z_i/Z_j\}) \equiv \frac{C}{C_{\text{bcc}}} \frac{\overline{Z}f(\{Z_i\})}{\overline{Z^{5/3}}} > 1$$

  where $f(\{Z_i\})$ is the dimensionless lattice structure function of the compound and C the corresponding structure constant.
  Chamel & Fantina, Phys. Rev. C94, 065802 (2016).

Ordered vs disordered compounds

Amorphous solids in accreted crusts are disfavored by observations of SXT. Nonaccreted crusts are unlikely to be less ordered.
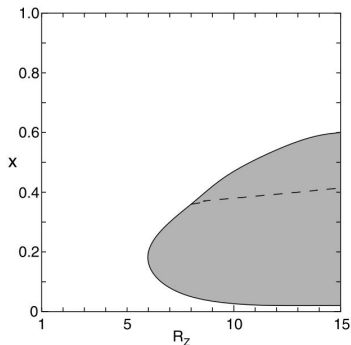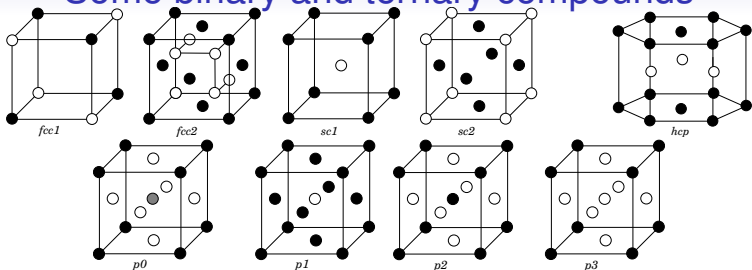

Stability of disordered binary Coulomb compounds with charge ratios $R_Z = Z_2/Z_1$ and composition $x = N_2/N$ against phase separation (shaded area)

Igarashi, Nakao, and Iyetomi, Contrib. Plasma Phys. 41, 319 (2001).

For the charge ratios expected in nonaccreted neutron-star crusts, disordered compounds are unstable.

Some binary and ternary compounds

Terrestrial examples:

- fcc1: rocksalt (NaCl), oxydes (MgO), carbonitrides (TiN)
- fcc2: fluorite (CaF_2)
- sc1: cesium chloride (CsCl), β-brass (CuZn)
- sc2: auricupride ($AuCu_3$)
- hcp: tungsten carbide (WC)
- p0: perovskite ($BaTiO_3$)

Stellar vs terrestrial compounds: (i) they are made of nuclei; (ii) electrons form an essentially uniform relativistic Fermi gas.

Substitutional compounds in neutron-star crusts

Compounds with CsCl structure are present at interfaces if $Z_1 \neq Z_2$.
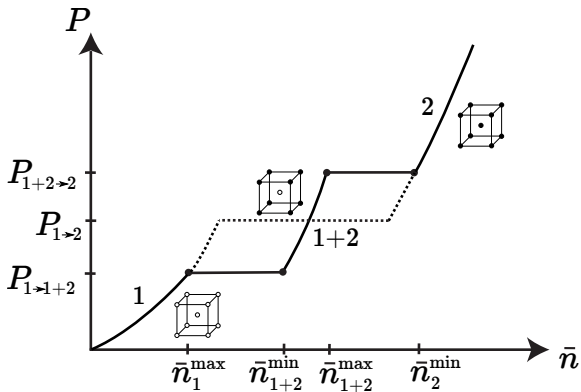
But they only exist over an extremely small range of pressures.
Chamel&Fantina, Phys. Rev. C94, 065802 (2016).

Outer crust of accreted neutron stars
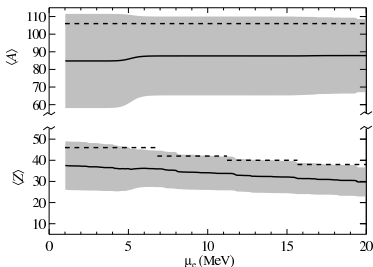
Accreted crusts are not in full thermodynamic equilibrium.

- The composition depends on the nuclear processes during X-ray (super)bursts.
- Ashes may be further processed (electron captures, pycnonuclear reactions) as they sink deeper inside the star.

— *Gupta et al.(2007)*

- - - *Haensel&Zdunik(2003)*

Different approaches:

- one-component liquid drop models
  Haensel&Zdunik, A&A404, L33 (2003)
  Haensel&Zdunik, A&A480, 459 (2008)
- multicomponent liquid drop models
  Steiner, Phys.Rev.C85, 055804 (2012)
- reaction networks
  Gupta et al., ApJ662, 1188(2007)

Impact of a high magnetic field on the crust?

In a high magnetic field $\vec{B}$ (along let's say the *z*-axis), the **electron motion perpendicular to the field is quantized into Rabi levels**:

$$e_\nu = \sqrt{c^2 p_z^2 + m_e^2 c^4 (1 + 2\nu B_\star)}$$

where $\nu = 0, 1, 2...$ and $\mathbf{B_\star} = \mathbf{B}/\mathbf{B_c}$

with $\mathbf{B_c} = \dfrac{\mathbf{m_e^2 c^3}}{\hbar \mathbf{e}} \simeq \mathbf{4.4 \times 10^{13}}$ G.

Rabi, Z.Phys.49, 507 (1928).

Maximum number of occupied levels for HFB-21:

$B_\star$	1500	1000	500	100	50	10	1
ν_{max}	1	2	3	14	28	137	1365

Electron quantization impacts the properties of the outer crust.
Chamel et al.,Phys.Rev.C86, 055804(2012)
Nandi&Bandyopadhyay, J.Phys.Conf.Ser.420, 012144 (2013)
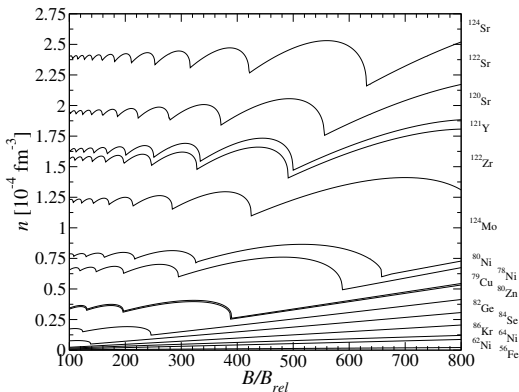*Basilico et al., Phys.Rev. C92, 035802 (2015)*

Composition of the outer crust of a magnetar

The composition depends on **B**, but not the structure (bcc).
Kozhberov, Astrophys. Space Sci.361, 256 (2016)

Equilibrium nuclides for HFB-24 and $B_\star \equiv B/(4.4 \times 10^{13}$ G):

Nuclide	$B_\star$
^{58}Fe(-)	9
^{66}Ni(-)	67
^{88}Sr(+)	859
^{126}Ru(+)	1031
^{80}Ni(-)	1075
^{128}Pd(+)	1445
^{78}Ni(-)	1610
^{79}Cu(-)	1617
^{64}Ni(-)	1668
^{130}Cd(+)	1697
^{132}Sn(+)	1989

Chamel et al., Progress in Theoretical Chemistry & Physics (Springer, 2017), pp 181-191.

Composition of the outer crust of a magnetar

High enough magnetic fields can change the structure of nuclei.
Pena Arteaga et al.,PRC84,045806(2011)
Stein et al.,PRC94,035802(2016)
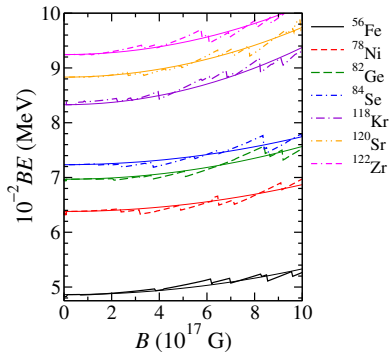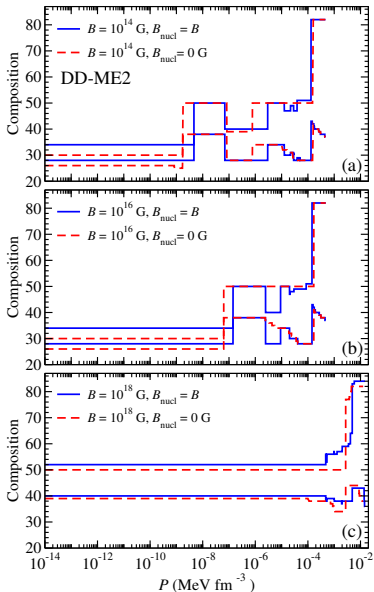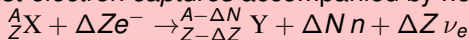

Right: crust composition obtained for a *reduced* set of nuclei.

Basilico et al., Phys.Rev. C92, 035802 (2015)

Neutron-drip transition: general considerations

Nuclei are actually stable against neutron emission but are unstable against *electron captures* accompanied by neutron emission

$$^A_Z X + \Delta Z e^- \rightarrow ^{A-\Delta N}_{Z-\Delta Z} Y + \Delta N\, n + \Delta Z\, \nu_e$$

- **nonaccreting neutron stars**
  All kinds of reactions are allowed: the ground state is reached for $\Delta Z = Z$ and $\Delta N = A$

	outer crust	drip line	$\rho_{\rm drip}$ (g cm^{-3})	$P_{\rm drip}$ (dyn cm^{-2})
HFB-19	^{126}Sr (0.73)	^{121}Sr (-0.62)	4.40×10^{11}	7.91×10^{29}
HFB-20	^{126}Sr (0.48)	^{121}Sr (-0.71)	4.39×10^{11}	7.89×10^{29}
HFB-21	^{124}Sr (0.83)	^{121}Sr (-0.33)	4.30×10^{11}	7.84×10^{29}

- **accreting neutron stars**
  Multiple electron captures are very unlikely: $\Delta Z = 1$ ($\Delta N \geq 1$)

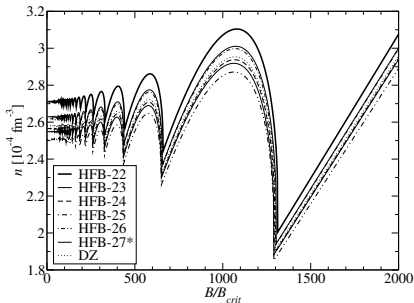 | | $\rho_{\rm drip}$ (g cm^{-3}) | $P_{\rm drip}$ (dyn cm^{-2}) |
  |---|---|---|
  | HFB-21 | $2.83 - 5.84 \times 10^{11}$ | $4.79 - 12.3 \times 10^{29}$ |

$\rho_{\rm drip}$ and $P_{\rm drip}$ can be expressed by simple analytical formulas.
Chamel et al., Phys.Rev.C91,055803(2015).

Neutron-drip transition in magnetars

The neutron drip density exhibits typical quantum oscillations.

Example using HFB-24:

These oscillations are almost universal:

$$\frac{n_{\text{drip}}^{\min}}{n_{\text{drip}}(B_\star = 0)} \approx \frac{3}{4}$$

$$\frac{n_{\text{drip}}^{\max}}{n_{\text{drip}}(B_\star = 0)} \approx \frac{35 + 13\sqrt{13}}{72}$$

In the strongly quantizing regime,

$$n_{\text{drip}} \approx \frac{A}{Z} \frac{\mu_e^{\text{drip}}}{m_e c^2} \frac{B_\star}{2\pi^2 \lambda_e^3} \left[1 - \frac{4}{3} C\alpha Z^{2/3} \left(\frac{B_\star}{2\pi^2} \right)^{1/3} \left(\frac{m_e c^2}{\mu_e^{\text{drip}}} \right)^{2/3} \right]$$

Chamel et al.,Phys.Rev.C91, 065801(2015).

Chamel et al.,J.Phys.:Conf.Ser.724, 012034 (2016).

Neutron-drip transition in magnetars

The neutron drip density exhibits typical quantum oscillations.

Example using HFB-24:

These oscillations are almost universal:

$$\frac{n_{\text{drip}}^{\min}}{n_{\text{drip}}(B_\star = 0)} \approx \frac{3}{4}$$

$$\frac{n_{\text{drip}}^{\max}}{n_{\text{drip}}(B_\star = 0)} \approx \frac{35 + 13\sqrt{13}}{72}$$

In the strongly quantizing regime,

$$n_{\text{drip}} \approx \frac{A}{Z} \frac{\mu_e^{\text{drip}}}{m_e c^2} \frac{B_\star}{2\pi^2 \lambda_e^3} \left[1 - \frac{4}{3} C\alpha Z^{2/3} \left(\frac{B_\star}{2\pi^2} \right)^{1/3} \left(\frac{m_e c^2}{\mu_e^{\text{drip}}} \right)^{2/3} \right]$$
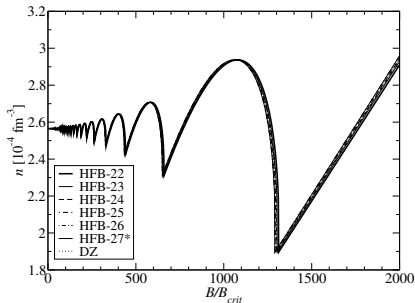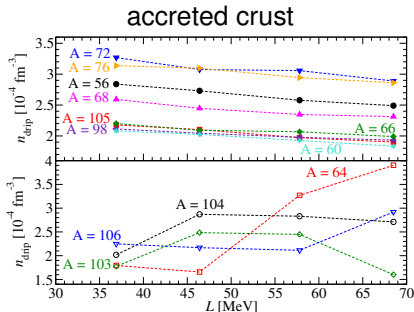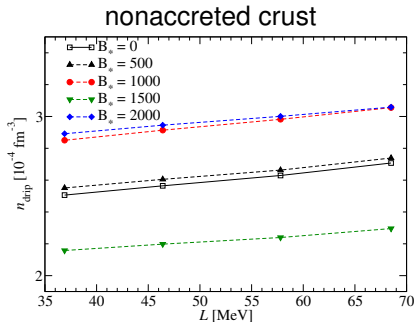
Chamel et al.,Phys.Rev.C91, 065801(2015).

Chamel et al.,J.Phys.:Conf.Ser.724, 012034 (2016).

Neutron-drip transition: role of the symmetry energy

The lack of knowledge of the symmetry energy translates into uncertainties in the neutron-drip density:
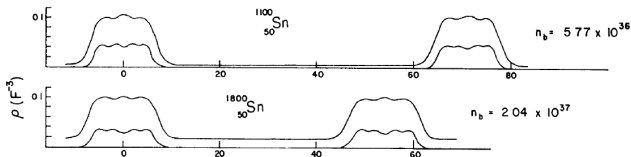

nonaccreted crust

accreted crust

Fantina et al.,Phys.Rev.C93,015801(2016)

In accreted crusts, the neutron-drip transition may be more sensitive to nuclear-structure effects than the symmetry energy.

Description of the inner crust of a neutron star

The conditions prevailing in the inner crust of a neutron star cannot be reproduced in terrestrial laboratories:

Negele&Vautherin,Nucl.Phys.A207,298(1973)

- The **neutron-saturated clusters** owe their existence to the presence of a highly degenerate surrounding neutron liquid.
- Unbound neutrons are expected to be **superfluid** at $T \leq T_c$ by forming Cooper pairs analogously to electrons in conventional superconductors.

State-of-the-art calculations rely on the self-consistent **nuclear energy density functional theory**.
Duguet, Lect. Notes Phys. 879 (Springer-Verlag Berlin Heidelberg, 2014), pp 293-350.

Pulsar sudden spin-ups and superfluidity

Neutron-star superfluidity was predicted by Migdal, and first studied by Ginzburg & Kirzhnits **before the discovery of pulsars**.
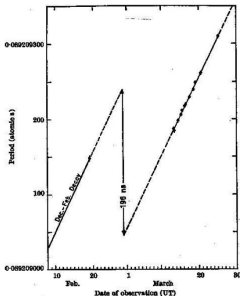
Some pulsars have been found to suddenly spin up (in less than a minute).

482 glitches have been detected in 168 pulsars.
http://www.jb.man.ac.uk/pulsar/glitches.html

Pulsar glitches provide the strongest evidence of superfluidity in neutron-star crusts.

Superfluidity may leave its imprint on other phenomena, e.g. thermal relaxation of SXT, QPOs in SGRs.

Some recent reviews:
Haskell&Sedrakian, arXiv:1709.10340 - White Book COST NewCompStar
Chamel, J. Astrophys. Astr.38, 43 (2017) - special issue in honor of Prof. Srinivasan

Nuclear energy density functional theory in a nut shell

The energy E of a nuclear system ($q = n, p$ for neutrons, protons) is expressed as a (universal) functional of

- $n_q(\boldsymbol{r}, \sigma; \boldsymbol{r'}, \sigma') = <\Psi|c_q(\boldsymbol{r'}\sigma')^\dagger c_q(\boldsymbol{r}\sigma)|\Psi>$
- $\widetilde{n}_q(\boldsymbol{r}, \sigma; \boldsymbol{r'}, \sigma') = -\sigma' <\Psi|c_q(\boldsymbol{r'} - \sigma')c_q(\boldsymbol{r}\sigma)|\Psi>$,

where $c_q(\boldsymbol{r}\sigma)^\dagger$ and $c_q(\boldsymbol{r}\sigma)$ are the creation and destruction operators for nucleon q at position $\boldsymbol{r}$ with spin $\sigma = \pm 1$.

In turn, these matrices are expressed in terms of **independent quasiparticle** wavefunctions $\varphi_{1k}^{(q)}(\boldsymbol{r})$ and $\varphi_{2k}^{(q)}(\boldsymbol{r})$ as

$$n_q(\boldsymbol{r}, \sigma; \boldsymbol{r'}, \sigma') = \sum_{k(q)} \varphi_{2k}^{(q)}(\boldsymbol{r}, \sigma)\varphi_{2k}^{(q)}(\boldsymbol{r'}, \sigma')^*$$

$$\widetilde{n}_q(\boldsymbol{r}, \sigma; \boldsymbol{r'}, \sigma') = -\sum_{k(q)} \varphi_{2k}^{(q)}(\boldsymbol{r}, \sigma)\varphi_{1k}^{(q)}(\boldsymbol{r'}, \sigma')^* = -\sum_{k} \varphi_{1k}^{(q)}(\boldsymbol{r}, \sigma)\varphi_{2k}^{(q)}(\boldsymbol{r'}, \sigma')^*.$$

The *exact* **ground-state energy** is obtained by minimizing the functional $E[n_q(\boldsymbol{r}, \sigma; \boldsymbol{r'}, \sigma'), \widetilde{n}_q(\boldsymbol{r}, \sigma; \boldsymbol{r'}, \sigma')]$ under the constraint of fixed nucleon numbers (and completeness relations on $\varphi_{1k}^{(q)}(\boldsymbol{r})$ and $\varphi_{2k}^{(q)}(\boldsymbol{r})$).

Hartree-Fock-Bogoliubov equations

Constrained variations of the nuclear energy functional yield the **self-consistent Hartree-Fock Bogoliubov** (HFB) equations

$$
\sum_{\sigma'} \int d^3 r' \begin{pmatrix} h_q(\boldsymbol{r}, \sigma; \boldsymbol{r'}, \sigma') & \widetilde{h}_q(\boldsymbol{r}, \sigma; \boldsymbol{r'}, \sigma') \\ \widetilde{h}_q(\boldsymbol{r}, \sigma; \boldsymbol{r'}, \sigma') & -h_q(\boldsymbol{r}, \sigma; \boldsymbol{r'}, \sigma') \end{pmatrix} \begin{pmatrix} \psi_{1k}^{(q)}(\boldsymbol{r'}, \sigma') \\ \psi_{2k}^{(q)}(\boldsymbol{r'}, \sigma') \end{pmatrix}
$$
$$
= \begin{pmatrix} E_k^{(q)} + \mu_q & 0 \\ 0 & E_k^{(q)} - \mu_q \end{pmatrix} \begin{pmatrix} \psi_{1k}^{(q)}(\boldsymbol{r}, \sigma) \\ \psi_{2k}^{(q)}(\boldsymbol{r}, \sigma) \end{pmatrix},
$$

where μ_q are the chemical potentials, and the non-local fields are defined by

$$
h_q(\boldsymbol{r}, \sigma; \boldsymbol{r'}, \sigma') = \frac{\delta E}{\delta n_q(\boldsymbol{r}, \sigma; \boldsymbol{r'}, \sigma')}, \quad \widetilde{h}_q(\boldsymbol{r}, \sigma; \boldsymbol{r'}, \sigma') = \frac{\delta E}{\delta \widetilde{n}_q(\boldsymbol{r}, \sigma; \boldsymbol{r'}, \sigma')}.
$$

Margueron&Sandulescu, in Neutron Star Crust, Eds C. Bertulani and J. Piekarewicz
(Nova Science Publishers, New York, 2012), p.65

Limitation: the exact functional is unknown... One has to rely on **phenomenological functionals**.

Implementations of the HFB equations

Assuming the crust is a **perfect (bcc) crystal**, the HFB equations need to be solved only inside one Wigner-Seitz cell of the lattice.
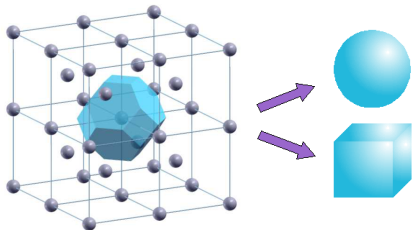
- **Wigner-Seitz approximation**
  Pastore et al., J.Phys.G44, 094003(2017)
  Grill et al., PRC84, 065801(2011)
  Baldo et al., PRC76, 025803(2007)

- **cubic box with periodic boundary conditions**
  Gögelein&Müther, PRC76, 024312 (2007)
  Magierski&Heenen,PRC65,045804(2002)

The crustal composition was found to depend on nuclear pairing.

But such calculations are limited by **spurious neutron shell effects**.

Fattoyev et al.,PRC95,055804(2017); Newton&Stone,PRC79,055801 (2009)
Margueron et al., in Exotic States of Nuclear Matter, Eds Lombardo, Baldo, Burgio, Schulze (World Scientific Publishing, 2008), p.362
Chamel et al., PRC75,055806(2007)

Implementations of the HFB equations

Going beyond:

Periodic boundary Condition

Wigner-Seitz cell   x (fm)   Supercell
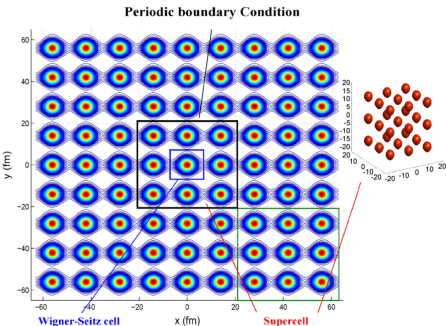
Sébille et al.,Nucl.Phys.A822,51(2009)

- **"Supercell"**
  Sébille et al., PRC 84, 055801 (2011)
  The results can be biased by the choice of the "supercell"
  Giménez Molinelli&Dorso,
  Nucl.Phys.A933,306 (2015)

- **Bloch boundary conditions**
  Schuetrumpf&Nazarewicz,PRC92,045806(2015)
  Chamel, PRC85,035801(2012)
  Requires the a priori knowledge of the crystal structure

Both approaches are computationally extremely costly: no systematic calculations of neutron-star crust matter so far

Semiclassical methods

Computationally very fast approximation of HFB equations based on an expansion of the smooth part of the single-particle density of states in powers of $\hbar$ (oscillatory part may be added perturbatively). This approach has been adapted to relativistic models.

Brack et al., Phys.Rep.123, 275 (1985)
Centelles et al., Ann.Phys.221, 165 (1993)

- **Extended Thomas-Fermi (4th order) + shell corrections (ETFSI)**
  Pearson et al., PRC91, 018801 (2015); Pearson et al.,PRC85,065803 (2012)
  Dutta et al.,PRC69,052801(R)(2004); Onsi et al.,PRC77,065805 (2008)

- **Extended Thomas-Fermi (2nd order)**
  Martin&Urban, PRC92, 015803 (2015)

- **Thomas-Fermi (zeroth order)**
  Lim&Holt, PRC95,065805 (2017); Fortin et al., PRC94,035804 (2016)
  Sharma et al., A&A 584, A103 (2015); Grill et al., PRC90, 045803 (2014)
 *Iida&Oyamatsu, EPJA50, 42 (2014); Okamoto et al., PRC88, 025801 (2013)*

Structure of nonaccreting neutron star crusts

With increasing density, the clusters keep essentially the same size but become more and more dilute.

Example of ETFSI calculations.

|	$\bar{n}_{cc}$ (fm^{-3})	P_{cc} (MeV fm^{-3})
BSk27*	0.0919	0.439
BSk25	0.0856	0.211
BSk24	0.0808	0.268
BSk22	0.0716	0.291
BSk21	0.0809	0.268
BSk20	0.0854	0.365
BSk19	0.0885	0.428
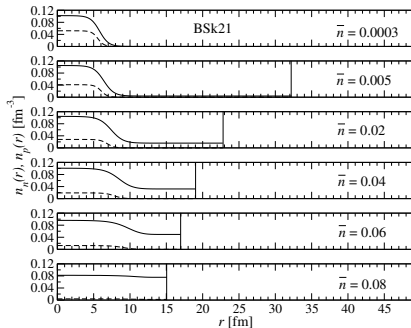
Chamel et al., Acta Phys.Pol.46,349(2015); Pearson et al., PRC91,018801(2015)
Pearson et al.,Phys.Rev.C85,065803(2012)

The crust-core transition is found to be very smooth.

Role of proton shell effects on the composition of the inner crust of a neutron star

- The ordinary nuclear shell structure seems to be preserved apart from $Z = 40$ (quenched spin-orbit?).
- The energy differences between different configurations become very small as the density increases!

ETF: dashed lines - ETFSI: solid lines
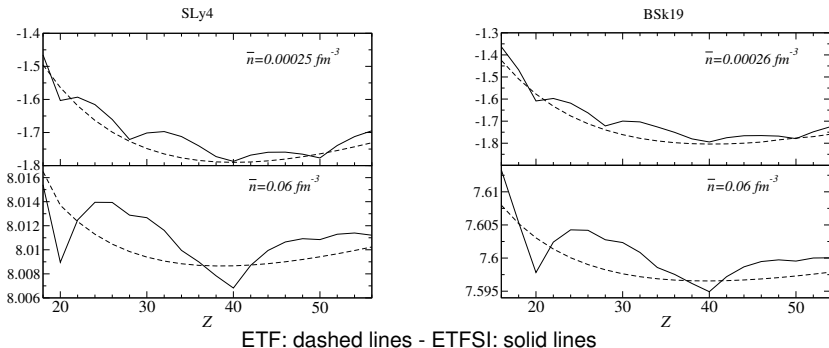
Role of proton pairing on the composition of the inner crust of a neutron star

Proton shell effects are washed out due to pairing.

Pearson et al., Phys.Rev.C91, 018801 (2015).
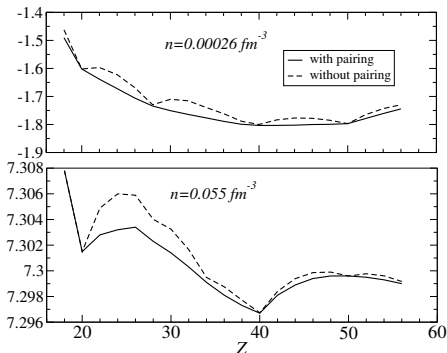
Example with BSk21.

At low densities, $Z = 42$ is energetically favored over $Z = 40$, but by less than 5×10^{-4} MeV per nucleon.

A large range of values of Z could be present in the deeper crust.

Due to proton pairing, the inner crust is expected to contain many impurities: calculations beyond the mean-nucleus approximation.
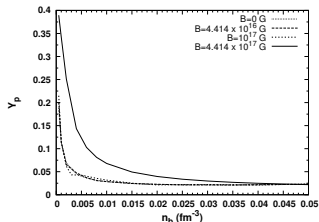
Role of a high magnetic field on the inner crust of a neutron star

- The neutron-drip transition is shifted to higher pressures
  Chamel et al.,Phys.Rev.C91, 065801(2015)

  Chamel et al.,J.Phys.:Conf.Ser.724, 012034 (2016)

- Neutron superfluidity is suppressed
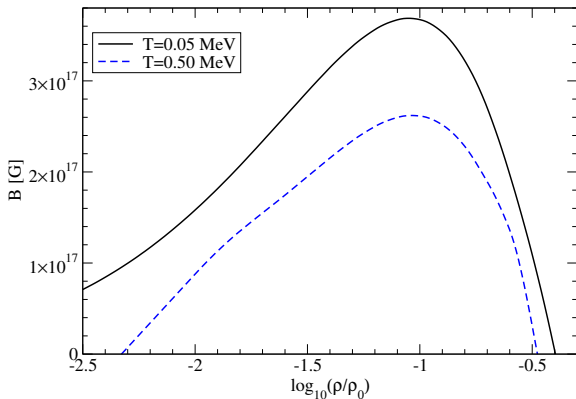
Stein et al., Phys.Rev.C93, 015802 (2016)

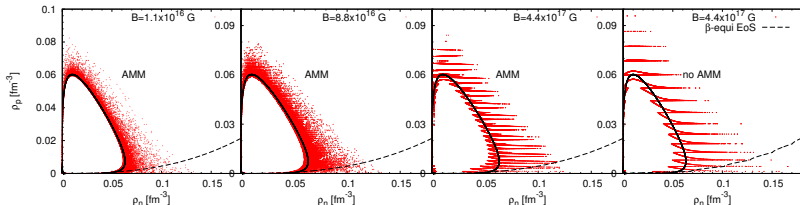# Role of a high magnetic field on the inner crust of a neutron star

Landau quantization of electron motion was studied in the TF approximation

- the neutron liquid is more dilute
- clusters are larger and closer
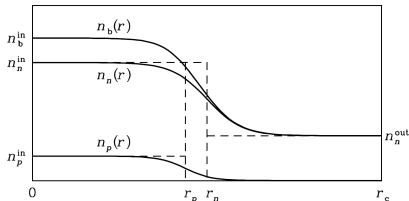
Nandi et al., ApJ736, 156 (2011)

Accounting as well for quantization of nucleon motion, the crust is expected to be **less neutron rich and highly heterogeneous**.

Chen, PRC95,035807(2017); Fang et al., PRC95,045802(2017)

Liquid drop models

Nuclear clusters and the neutron liquid are treated as two **distinct coexisting homogeneous phases**.

In principle, bulk and surface energies can be calculated from the EDF theory, but empirical parametrizations are often used.

Haensel, Potekhin, Yakovlev, Neutron Star: Equation of State and Structure (Springer, 2007)

- liquid-drop models allow for systematic studies
- they were used to show that the formation of clusters arise from a detailed balance between surface and Coulomb effects ("pastas")

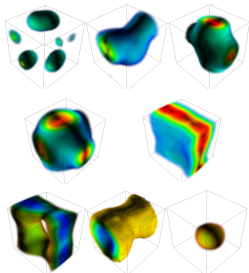*Lim&Holt, PRC95,065805 (2017); Tews et al., PRC95,015803 (2017)*
Fortin et al., PRC94,035804 (2016); Bao&Shen, PRC93,025807(2016)
Gulminelli&Raduta, PRC92,055803 (2015); Deibel et al., PRC90,025802 (2014)

Nuclear "pastas"

Nuclear "pastas" were first predicted based on liquid drop models.

*Ravenhall et al., PRL50, 2066 (1983); Hashimoto et al., PTP71, 320 (1984)*

Nuclear "pastas" have been studied using liquid-drop models, semiclassical methods, and nuclear EDF theory.

Chamel&Haensel, Liv. Rev. Relativ. 11 (2008), 10
Watanabe&Maruyama, in Neutron Star Crust, Eds Bertulani&Piekarewicz (Nova Science Publishers, 2012), p. 23

Schuetrumpf et al., PRC87, 055805 (2013)

In all these approaches, a few specific nuclear shapes are generally considered, or some symmetries are assumed.

The following sequence is expected with increasing nuclear volume fraction *w*:
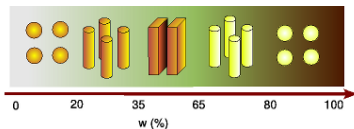
Nuclear "pasta" formation

The formation of nuclear pastas has been explored using large scale molecular dynamics in a box with periodic boundary conditions.
Dorso et al., in Neutron Star Crust, Eds Bertulani&Piekarewicz (Nova Science Publishers, New York, 2012), pp. 151-169.

- **classical molecular dynamics** ($N \sim 10^3 - 10^5$)
  pointlike particles interacting through a two-body potential
  Berry et al., PRC94,055801(2016); Dorso et al., PRC86,055805(2012)
- **quantum molecular dynamics** ($N \sim 10^3$)
  Gaussian wave packets moving (classically) in a mean field.
  Phenomenological antisymmetrisation (Pauli potential).
  Maruyama et al., Prog.Theor.Exp.Phys. 2012,01A201(2012)
- **fermionic molecular dynamics** (very costly, scale as N^4 vs N^2)
  Slater determinants.
  Vantournhout et al.,Prog.Part.Nucl.Phys.66,271(2011); Vantournhout&Feldmeier, J.Phys.Conf.Ser.342,012011(2012)

Results could be influenced by the geometry of the box and the treatment of Coulomb interactions.
Giménez Molinelli&Dorso,NPA933,306 (2015); Alcain et al., PRC89,055801(2014)

Nuclear "pasta" formation

As clusters get closer with increasing density, they eventually fuse and connect into herringbone structures turning into "spaghettis".

Watanabe et al., PRL103, 121101 (2009)
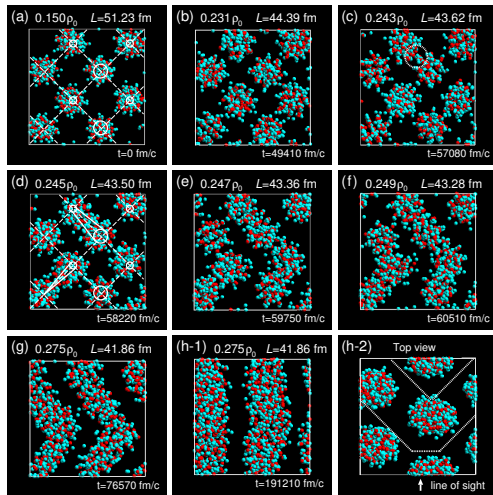
Nuclear cooking

All models supporting the existence of pastas predict the following sequence: gnocchi/polpette (spherical clusters), spaghetti (cylindrical clusters), lasagna (slabs), bucatini/penne/maccheroni (cylindrical holes), Swiss cheese/scaciatta (spherical holes).

Intermediate phases have been found by some models:

- **"nuclear waffles"** (slabs with holes)
  Schneider et al.,PRC90,055805 (2014)
  Sébille et al.,PRC84,055801(2011)
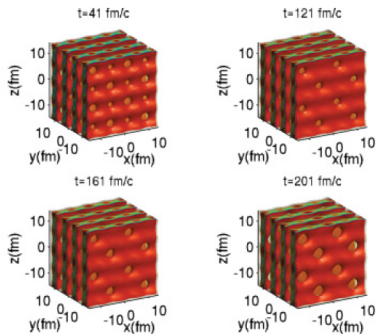 *Williams&Koonin,NPA 435, 844 (1985)*

- **cross-rods**
  Pais&Stone, PRL109,151101(2012)
  Lassaut et al.,A&A183,L3(1987)
  Williams&Koonin,NPA35,844(1985)

- **slabs connected by helical ramps**
  Berry et al.,PRC94,055801(2016)

Conclusions

Most studies of neutron-star crusts consider cold catalysed matter.

- **The ground state of the outer crust is fairly well known**: its composition is completely determined by (experimental) nuclear masses, and its structure is a bcc crystal.

- **The ground state of the inner crust is more uncertain** (nuclear pastas?)

- **The crust of neutron stars may not be fully catalysed** depending on the stellar evolution (impurities, defects).

- **The constitution of accreted crusts is very uncertain**: the composition depends on nuclear reactions during X-ray (super)bursts, and the burial of accreted matter; the structure depends on the evolution (compounds?).

- **Magnetars may have different crusts**: less compressible (condensed surface?), less neutron-rich (pure crust?), suppression of superfluidity